Direct Measurement of Single-Stranded DNA Translocation by PcrA Helicase Using the Fluorescent Base Analogue 2-Aminopurine†

Mark S. Dillingham,‡,§ Dale B. Wigley,‡ and Martin R. Webb*,‖

Imperial Cancer Research Fund, Clare Hall Laboratories, Blanche Lane, South Mimms, Potters Bar, Hertfordshire EN6 3LD, U.K., and National Institute for Medical Research, The Ridgeway, Mill Hill, London NW7 1AA, U.K.

Received June 1, 2001

ABSTRACT: Use of the fluorescent base analogue 2-aminopurine has provided a direct demonstration of the translocation of PcrA helicase toward the 5′-end of single-stranded DNA. Single 2-aminopurine bases are introduced into otherwise standard oligonucleotides and produce a fluorescence signal when PcrA reaches their position. We demonstrate that random binding of PcrA to ssDNA is followed by translocation in an ATP-dependent manner toward the 5′-terminus at 80 bases per second at 20 °C. The data also provide information on the kinetics of ssDNA binding to the helicase and of the protein dissociation from the 5′-end of ssDNA. A full kinetic model is presented for ATP-dependent DNA translocation by PcrA helicase.

DNA helicases are motor proteins involved in the regulation of DNA secondary structure (for reviews see refs *1*−*3*), a process essential in many aspects of DNA function. Consequently, DNA helicases are ubiquitous and may account for as much as 1% of the genome (*4*). Strictly speaking, DNA helicases are nucleoside triphosphatases that catalyze the separation of duplex DNA into its component single strands. However, many enzymes are identified as helicases on the basis of conserved sequence motifs but are actually involved in more diverse processes such as Holliday junction progression and the processing of stalled replication forks (*5*). Indeed, it has been suggested that the "helicase" protein motifs may be indicative of DNA translocases rather than helicases per se (*6*).

The helicase in this study is PcrA, an essential protein of Gram-positive organisms where it has a role in DNA repair and plasmid rolling circle replication (*7*, *8*). It is a member of helicase superfamily I and is closely related to the well-studied Rep, UvrD, and RecB(CD) helicases from *Escherichia coli*. Structural and biochemical analyses of PcrA support a model in which the protein functions as a monomer using an "inchworm"-type mechanism to translocate DNA and separate the complementary strands (*6*, *9*−*11*). The protein binds and distorts the duplex DNA in an ATP-dependent manner (*6*, *11*). However, processive helicase activity requires a structurally distinct region that binds single-stranded DNA (ssDNA)[1] as part of a DNA tracking motor. This motor requires the hydrolysis of one ATP molecule for the movement of the distance equivalent to one base (*10*). The ssDNA binding is accomplished largely by a series of individual base binding sites, each with aromatic interactions with the protein (*6*). A detailed molecular mechanism for the motor was proposed in which these protein−base binding sites are modulated during the ATP hydrolysis cycle. Sites are created and removed by conformation changes imposed by various ATPase nucleotide states, resulting in protein movement relative to ssDNA in the 3′- to 5′-direction.

Various types of proteins have been identified which may be capable of active translocation on DNA. Of these, several classes contain the helicase motifs including five groups of helicases, type I restriction enzymes, and chromatin remodeling enzymes (*3*, *4*). Other enzymes displaying DNA translocation activity include DNA polymerases and proteins involved in DNA transport, such as phage packaging or chromosome segregation (*12*, *13*).

Here we describe a fluorescence method to study protein translocation on DNA. Although, in general, there are limited methods to monitor protein motion along DNA, for particular systems considerable progress has been made. For instance, DNA translocation in the type I restriction enzymes has been studied using a phage packaging technique (*14*), a triplex displacement assay (*15*), and by direct observation with atomic force microscopy (*16*). In the DNA helicases, an elegant demonstration of RecBCD helicase/nuclease translocation has recently been provided by the direct observation of the activity of a single protein molecule on λ DNA (*17*). With this exception, all other measurements of DNA helicase-catalyzed DNA translocation have been indirect. Unidirectional ssDNA translocation by PcrA helicase has been studied by analysis of pre-steady-state ATP hydrolysis kinetics (*10*). Other techniques have included studying the

† This work was supported by the Wellcome Trust (M.S.D. and D.B.W.) and the Medical Research Council, U.K. (M.R.W.).

* To whom correspondence should be addressed. Phone: (44) 20 8959 3666 2078. Fax: (44) 20 8906 4477. E-mail: mwebb@nimr.mrc.ac.uk.

‡ Imperial Cancer Research Fund, Clare Hall Laboratories.

§ Current address: Section of Microbiology, University of California at Davis, Hutchison Hall, Davis, CA 95616.

‖ National Institute for Medical Research.

[1] Abbreviations: ssDNA, single-stranded DNA; 2AP, 2-aminopurine. The term 10_{2AP} is used for the oligonucleotide, 5′-2AP-TTTTTTTTT-3′; other oligonucleotides are abbreviated similarly.

10.1021/bi011137k CCC: $22.00
Published on Web 12/13/2001

DNA dependence of the ATPase activity (*18*, *19*), investigating the effects of static blocking agents (*20*−*22*), and demonstrating displacement of streptavadin from biotin-labeled oligonucleotides (*23*). Study of translocation by PriA helicase has made use of its unusual property of starting from a defined sequence on DNA (*24*), whereas most helicases, including PcrA, are nonspecific for sequence.

In this study we describe the interaction of PcrA with ssDNA containing the fluorescent base 2-aminopurine (2AP). 2AP is a close analogue of adenine and is capable of forming base pairs with thymine. It causes minimal distortion to a DNA duplex structure (*25*, *26*). The fluorescence properties of 2AP in duplex DNA have been used previously to study many protein−DNA interactions including base flipping by uracil DNA glycosylases (*27*) and DNA methyltransferases (*28*, *29*) and promoter interaction and nucleotide incorporation by polymerases (*30*). The fluorescent base has also been used to report the separation of duplex DNA into its component single strands by DNA helicases (*31*). In this present study, the fluorescence signal is used as a reporter of the position of PcrA relative to a 2AP base incorporated within an otherwise standard single-stranded oligonucleotide. This makes use of a fluorescence increase which occurs when the 2AP moiety is bound within the ssDNA binding site of PcrA. Using a rapid reaction technique to follow the fluorescence changes in real time, it is possible to measure protein motion on ssDNA, as well as association and dissociation of PcrA and the DNA.

We have previously described a kinetic model for ssDNA translocation by PcrA helicase based on measurements of pre-steady-state P_i release from PcrA·DNA complexes (*10*). In this model, PcrA binds randomly to DNA before translocating toward the 5′-end. Dissociation from the DNA is slow, resulting in the accumulation of the helicase at the DNA 5′-terminus. This idea provided the rationale for the translocation experiments reported here. If a 2-aminopurine base (2AP) is substituted suitably at the 5′-terminus of the ssDNA in place of a natural base, then it should provide a signal to observe the translocation process more directly. Furthermore, data can be obtained for binding and dissociation of PcrA and 2AP-substituted DNA, using the concomitant fluorescence changes. These data were used to develop the kinetic mechanism of the ATP-dependent translocation.

EXPERIMENTAL PROCEDURES

Protein and Oligonucleotides. *Bacillus stearothermophilus* PcrA was prepared as described previously (*8*). All oligonucleotides, including those containing 2AP, were synthesized and HPLC-purified by Oswel Ltd. (Southampton, U.K.). Protein and DNA concentrations were determined by spectrophotometry using calculated extinction coefficients. The data presented in this paper are for oligonucleotides containing 2AP as the 5′-terminal base, with all other bases being thymine.

Fluorescence Stopped-Flow Measurements. These were made with a HiTech SF61MX apparatus with excitation at 313 nm through 5 mm slits and emission measured after a 360 nm cutoff filter. All concentrations quoted are final ones after mixing and, unless stated otherwise, were 500 nM PcrA, 2.5 μM 2AP-substituted oligonucleotide, and 500 μM ATP. Previous experiments (*10*, *32*) have shown that this ATP concentration is saturating, and this was confirmed empirically. For DNA chase and DNA dissociation experiments, 25 μM dT_{50} was used to sequester PcrA molecules after dissociation from 2AP oligonucleotides. A 5-fold 2AP oligonucleotide to protein ratio was used throughout to ensure that most protein−DNA complexes contained a single PcrA monomer bound to each oligonucleotide, while still allowing good signals during experiments. Experiments were performed at 20 °C in a buffer containing 50 mM Tris·HCl, pH 7.5, 150 mM NaCl, and 3 mM $MgCl_2$. The translocation data presented are the average of up to three traces. Kinetic data were fitted using the Hitech software, Grafit (*33*) and Scientist (MicroMath, Salt Lake City, UT). Kinetic simulations were performed using the program ModelMaker version 3 (Cherwell Scientific, Oxford, U.K.).

RESULTS

A prerequisite of using 2AP-substituted DNA is to know to what extent the modified base affects the activity of PcrA. There is unlikely to be a large effect, because PcrA-catalyzed DNA translocation is insensitive to natural base composition (*10*). The pre-steady-state kinetics of P_i release from PcrA provide a sensitive measure of DNA translocation and dissociation (*10*). Using this criterion, a direct comparison was made between oligo-T and equivalent oligonucleotides with a 2AP substituted either in the middle or at the 5′-end. The presence of 2AP in the oligonucleotide had no effect on the P_i release traces (data not shown).

PcrA Association Kinetics Measured with 2AP Oligonucleotides. A fluorescence intensity change occurs on binding PcrA to short single-stranded 2AP oligonucleotides in the absence of ATP. However, the fluorescence excitation spectra of 2AP and tryptophan overlap, so 313 nm was chosen for excitation as relatively very little excitation of PcrA tryptophan occurs at this wavelength. This was shown by control experiments in the absence of 2AP, and an example is described later (Figure 7). Using this wavelength, it was shown that essentially all fluorescence was due to the 2AP rather than tryptophan.

The binding kinetics were measured for a variety of synthetic oligonucleotides of different lengths, incorporating a single 2AP at various positions. However, all data presented here are for oligonucleotides containing a 2AP at the 5′-terminus as it is these oligonucleotides that are used in the translocation experiments described below. Similar DNA binding curves are obtained if the 2AP is incorporated at other positions (data not shown).

For the 10-base oligonucleotide 10_{2AP}, which has 2AP as the 5′-terminal base, PcrA binding was accompanied by a fluorescence increase of up to 16% (Figure 1a). Given the 5-fold excess of 10_{2AP} over protein, the fluorescence change for binding one PcrA to one 10_{2AP} is 80%. Because of random binding, there are several possible binding sites on the DNA, but only some will give rise to this increase. So the fluorescence enhancement on PcrA binding the 2AP is severalfold, and we will return to this point later. Binding kinetics were measured over a range of concentrations of 10_{2AP} and were well fit to single exponentials. The rate increased hyperbolically with concentration and did not change significantly at >5 μM (Figure 1b), so the data were

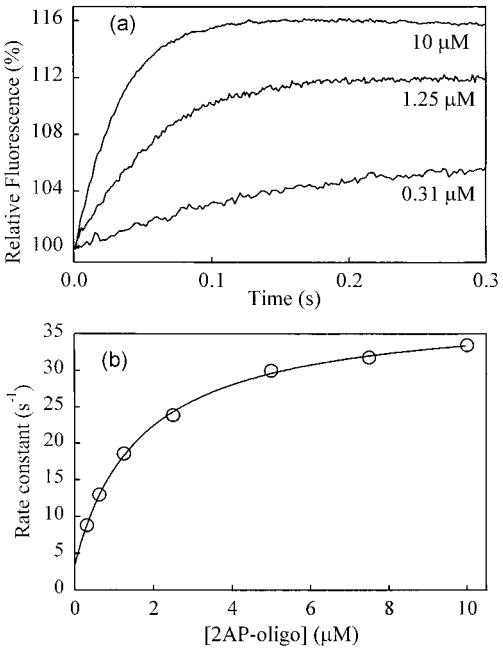

FIGURE 1: Association kinetics for PcrA with 10_{2AP}. Experiments were performed at 20 °C as described in Experimental Procedures. (a) Fluorescence signal for PcrA binding to 10_{2AP} at the concentrations indicated. PcrA was at 20% the concentration of DNA. The data were fit to single exponentials. (b) Relationship between observed rate of association and concentration of 10_{2AP}. The curve is the best fit to a hyperbola; see text for details.

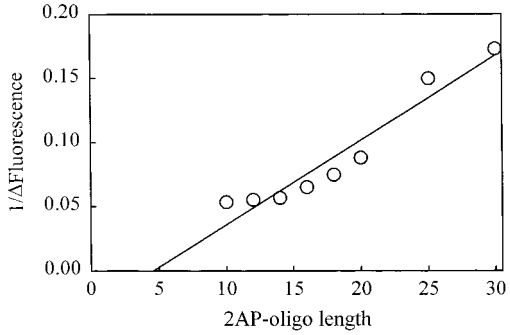

FIGURE 2: Fluorescence increases on PcrA binding to 5′-2AP oligonucleotides as a function of oligonucleotide length. The data were obtained as described in the text and are plot as reciprocal percentage increases. They are fitted to the reciprocal of eq 2.

fit to a simple two-step binding model:

$$\text{PcrA} + \text{DNA} \overset{1}{\rightleftharpoons} \text{PcrA·DNA} \overset{2}{\rightleftharpoons} \text{PcrA·DNA*} \qquad (1)$$

Step 1 is rapid bimolecular binding. Step 2 is accompanied by the fluorescence change to give a high fluorescence state, indicated by the asterisk. The forward, reverse rate constants and equilibrium constant for any step i are designated k_i, k_{-i}, and K_i, respectively. The fit gives $1/K_1$ as 1.7 μM and $k_{+2} + k_{-2}$ as 35 s^{-1}.

These binding measurements were repeated with oligonucleotides of different length, and the fluorescence change on binding was determined from the amplitudes of traces equivalent to Figure 1. The measurements were done at saturating concentrations of DNA, so that the maximum possible fluorescence change and rate were obtained. As the length increases, this fluorescence change becomes progressively smaller (Figure 2). The change on binding PcrA to 50_{2AP} is barely detectable (data not shown). This is presumably because most of the protein binds at sites along the DNA well away from the 2AP at the 5′-end. Following the rapid binding there is a slow, small exponential decrease in fluorescence (illustrated in Figure 6, where a binding trace will be shown on a much slower time scale). This may be due to a small redistribution of PcrA along the DNA, if binding at the 5′-end is unfavored thermodynamically, so that slow equilibration leads to preferred binding at sites away from the ends.

The model of initial random binding is supported by the data as shown in Figure 2. The fit to the data assumes that only a few binding sites at the 5′-end give rise to the fluorescence change: the modeling, described later, will assume that binding at 3 neighboring sites gives rise to the enhanced fluorescence. The observed change is therefore dependent on the total number of binding sites. As assumed in analyzing the P_i release data (*10*), the number of available binding sites is $n - x$, where n is the number of bases. The fixed number x takes into account the fact that the PcrA covers several bases but that the protein may overhang the end of the DNA partially without significant decrease in binding constant: the number of available, distinct binding sites is less than the number of bases. Note that the parameter x does not give an estimate of the total width of the PcrA binding site because of this possible overhang. In other words, the span of the protein in terms of length of oligonucleotide bases is different from the minimum number of bases that need to be bound for viable interaction. Note that these numbers may be different from the shortest oligonucleotide that can bind, since this final number depends on an assessment of what tightness of binding is viable. The observed fluorescence enhancement is therefore given by

$$\Delta F_{obs} = \Delta F_{max}/(n - x) \qquad (2)$$

where ΔF_{max} is the fluorescence enhancement when all PcrA binds only to site(s) producing enhancement (i.e., a very short oligonucleotide). Figure 2 suggests that $x = 4$, which, given the likely errors in Figure 2, is not statistically different from the value of 2 obtained from the P_i release measurements, using the same definition for x (*10*). For 10_{2AP}, this would mean that there are six to eight overlapping sites for PcrA binding. However, this measurement does not give an estimate of the proportion of these sites that contribute to fluorescence enhancement, although multiple fluorescent sites would lead to the deviation from linearity that we observe for short oligonucleotides. It should also be noted that because the fluorescence enhancement is very low at long oligonucleotides, the error in the reciprocal is large.

Dissociation of PcrA from 10_{2AP}. Dissociation kinetics in the absence of ATP were measured by mixing the PcrA·10_{2AP} complex with a large excess of unlabeled DNA (Figure 3). There was an exponential decrease in fluorescence at 1.3 s^{-1}, and this was followed by a very slow linear decrease. Presumably the exponential decrease represents dissociation of PcrA that had been bound at the 5′-end and is equivalent to k_{-2} in eq 1. This change has a smaller amplitude than found for binding, in line with the suggestion that in the preformed complex there is time for a redistribution of PcrA along the DNA.

The slow linear fluorescence decrease might, in principle, be photobleaching. However, traces from other types of

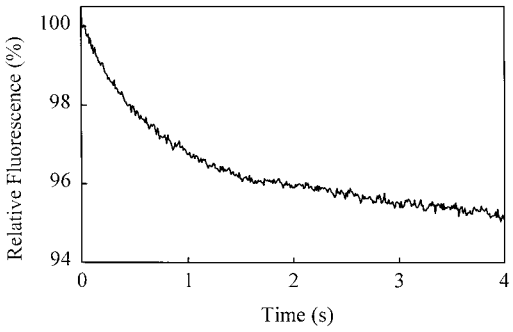

FIGURE 3: Dissociation kinetics of PcrA and 10_{2AP}. This was measured by rapidly mixing PcrA·10_{2AP} with a large excess dT_{50}; see text for details.

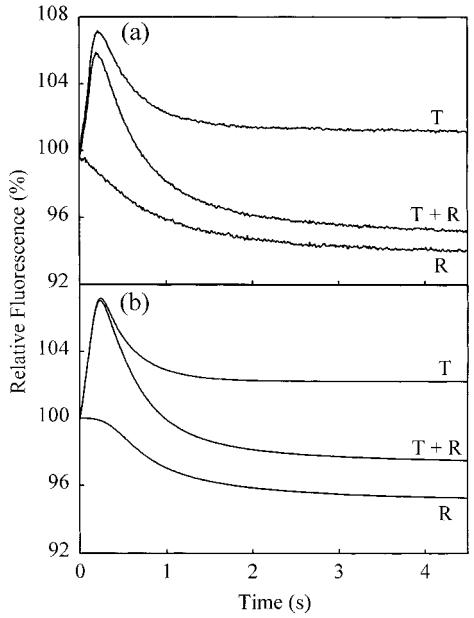

FIGURE 4: Fluorescence changes associated with PcrA translocation along 20_{2AP}. The translocation of 0.5 μM PcrA along 2.5 μM 20_{2AP} was initiated by 500 μM ATP. (a) The traces are for the preformed PcrA·20_{2AP} complex mixed rapidly with ATP in the absence (T) or presence (T + R) of chase dT_{50}. Trace R is the difference between these and represents dissociation. (b) The simulation of these curves using the mechanism in Figure 8. See text for details.

measurement over a similar time scale (e.g., Figures 4a and 7) do not show this decrease. The decrease may be a further relaxation, for example, involving slow movement of other PcrA molecules along the DNA, prior to dissociation. Alternatively, it may be due to dissociation of PcrA bound close to but not right at the 5′-end that could still generate a fluorescence enhancement while bound. Thus the observed rate constant may reflect the fact that binding right at the 5′-end of the DNA is weaker than in the central part. This idea would also explain the slow decrease in fluorescence seen in the binding traces (Figure 1). Rapid random binding would be followed by slow redistribution to thermodynamically more favored sites, which are distant from the 2AP.

DNA Translocation. The relationship between 2AP fluorescence and DNA translocation was investigated by rapidly mixing PcrA with a 5-fold excess of 2AP oligonucleotide and saturating quantities of ATP. When the preformed PcrA·20_{2AP} complex was mixed with ATP, the fluorescence trace consisted of two main phases (Figure 4). An approximately linear fluorescence increase to a maximum was followed by an exponential decrease to a final constant value. These fluorescence changes were not observed if ATP was absent, and this will be presented later with other controls.

The time of the maximum fluorescence approximately coincides with the end of the rapid P_i release phase in the ATPase measurements (*10*). In our determination of the step size of PcrA helicase (*10*), it had previously been assumed that this rapid phase of P_i release from PcrA·ssDNA complexes was linked to translocation to the 5′-end. As discussed later, this relationship is confirmed by the 2AP fluorescence experiments. We interpret the approximately linear fluorescence increase as a measure of movement of protein molecules to the 5′-end, from their initial positions randomly bound along the DNA. The fluorescence enhancement represents PcrA at the 5′-end, such that the 2AP can interact with the protein.

The exponential decrease at 2.3 s^{-1} represents a relaxation of the complex at the 5′-end as the overall reaction reaches steady state. This relaxation might include a component due to dissociation, and this was investigated by a chase experiment (Figure 4) in which a large excess of unlabeled DNA was present with the ATP and then mixed with the PcrA·20_{2AP} complex. Any dissociation of this complex is followed by association of PcrA with the unlabeled DNA, rather than with 2AP DNA. A fluorescence signal will accompany the dissociation. This addition of unlabeled DNA leaves the linear increase in fluorescence largely unchanged but causes considerable changes in the subsequent decrease in fluorescence. This is consistent with the linear increase being due to translocation prior to significant dissociation. The fluorescence decrease is now clearly biphasic. To analyze this, the two traces (chase and no chase) were subtracted, and the resultant trace was an approximately exponential decrease in fluorescence (Figure 4). This difference trace was fitted to a single exponential from the time of maximum fluorescence to give a rate of 1.0 s^{-1}. These data suggest that, in the absence of "chase" DNA, the final relaxation is largely due to a process while the PcrA remains bound at the 5′-end and there is not much net dissociation (i.e., the concentration of uncomplexed PcrA is low). Dissociation is followed by rapid reassociation and translocation, and so the rate is limited by the dissociation itself. The result of this is to have little effect on the fluorescence. However, in the presence of chase DNA, net dissociation from the 5′-end does occur as the presence of the chase DNA prevents the reassociation to the fluorescent DNA. The difference trace represents this net dissociation of the steady-state, 5′-bound complex.

There is not a large lag in this difference trace, and there is a small decrease in amplitude of the linear phase in the chase experiment relative to the simple translocation. These observations may indicate that there is some dissociation of PcrA from other sites along the DNA during translocation. We will discuss these points later.

Translocation measurements were repeated using oligonucleotides from 10 to 50 bases in length (Figure 5a). Note that for clarity the data are plotted as fluorescence *change* with time, and so the traces coincide at zero time. In practice, the absolute fluorescence of these preformed complexes differs at zero time because the fluorescence enhancement on complex formation changes with length. The rate of the fluorescence rise decreases with length of DNA with concomitant increase in the time to reach the maximum

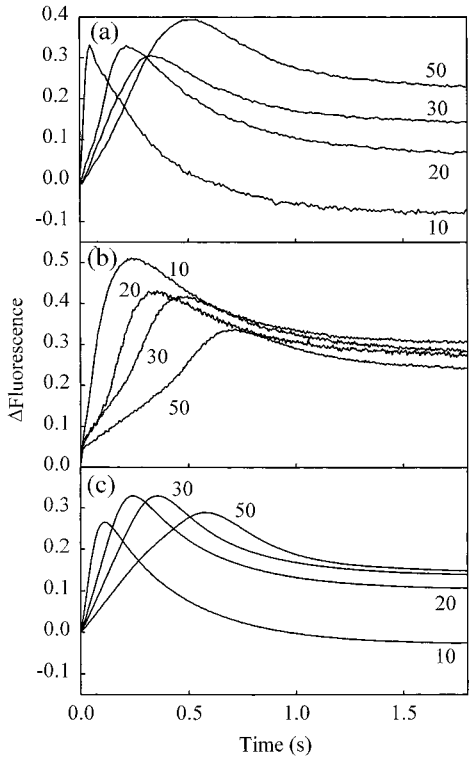

FIGURE 5: Fluorescence changes associated with PcrA translocation along 5′-2AP oligonucleotides of different lengths. Concentrations are as in Figure 4. The numbers refer to the length of oligonucleotides. (a) Preformed PcrA·DNA complexes were mixed rapidly with ATP. (b) PcrA was mixed with oligonucleotide and ATP. (c) Simulations of traces in (a) using the mechanism in Figure 8. See text for details.

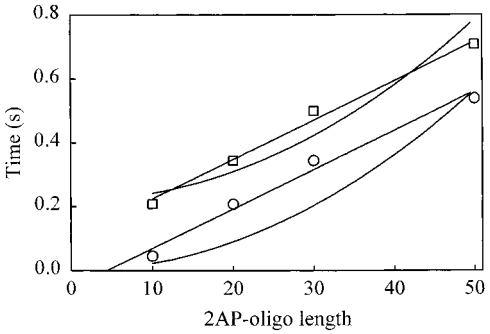

FIGURE 6: Relationship between the time of transient maximum fluorescence and length of oligonucleotide. Data are from Figure 5a (translocation only, circles) and 5b (binding and translocation, squares) and were fitted globally either linearly (unidirectional translocation) or parabolically (random walk) (*35*). The linear fit gives a slope of 0.0123 s per base. The line for translocation of the preformed complex intercepts the *x*-axis at 4.3 bases. The parabola was of the form time = a(base − b)^2 and time = a(base − b)^2 + c, where b and c must be positive. The best fit gave a = 0.219, b = 0, and c = 0.0002216.

fluorescence, while the rate of the final relaxation is largely unchanged. These observations are consistent with the idea that the linear phase represents PcrA translocation toward the 5′-end of the oligonucleotide. In that case, the time taken to reach peak fluorescence is linearly related to the distance translocated by the PcrA molecules, i.e., the length of the oligonucleotide (Figure 6). The rates of the final phase are 2.3, 2.4, 2.3, and 2.9 s^{-1} for 10_{2AP}, 20_{2AP}, 30_{2AP}, and 50_{2AP}. The fact that the final phase is largely unaffected by length is consistent with it being due to a process occurring to the

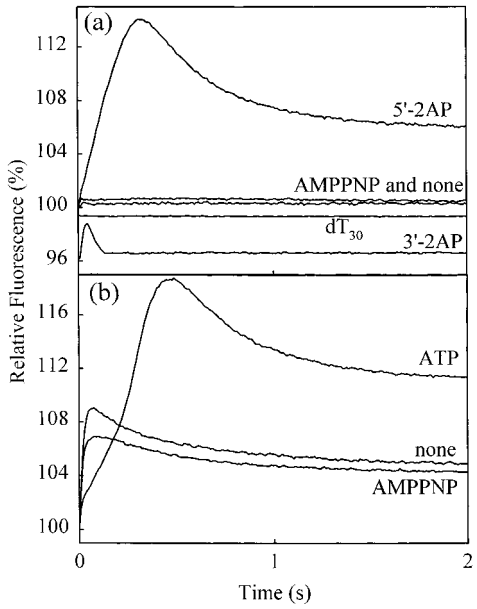

FIGURE 7: Controls for measurements of ATP-coupled PcrA translocation along 30-base oligonucleotides. Measurements were done as for Figures 4 and 5. (a) The PcrA·DNA complex was preformed. 5′-2AP is 30_{2AP} in the presence of 500 μM ATP. Traces are also shown with 500 μM AMPPNP or no nucleotide. 3′-2AP is the equivalent measurement using a 30mer with 2AP at the 2-position and all other bases T. This trace is offset by ~30%, as the uncomplexed oligonucleotide is less fluorescent than those with 2AP right at the 5′-end. The measurement with dT_{30} had the instrument setting exactly as the others. The signal was ~10% of that for 30_{2AP}, and so the traces has been offset by 90%. The 10% signal was almost entirely due to scatter, as the signal without oligonucleotide or protein was also 10%. (b) Traces from mixing 30_{2AP} with PcrA in the presence of ATP, AMPPNP, or no nucleotide.

complex bound at the 5′-end. Using chase experiments the dissociation rates were measured as 2.2, 1.0, 1.0, and 0.94 s^{-1}, respectively, suggesting that the 10mer has more rapid dissociation than longer oligonucleotides.

Fluorescence was also measured in the stopped-flow apparatus after mixing PcrA with DNA plus ATP (Figure 5b). Now an additional rapid phase of small amplitude is observed compared with the traces when the complex is preformed. This is probably due to DNA binding. The subsequent fluorescence increase is now more complex, with a slow change that then accelerates. This is then followed by a slow relaxation as before. The differences in the rising fluorescence from those with the preformed complex may reflect processes following binding but before translocation, as described in the modeling. These data are again plotted as changes in fluorescence, but now the values at zero time are for unbound 2AP oligonucleotide and so are essentially unaffected by length. The final fluorescence levels are also very similar, indicating that the final species are also not affected by length. For both sets of data (Figure 5a,b) a linear relationship is observed between the time taken to reach peak fluorescence and the length of oligonucleotide (Figure 6).

Figure 7 shows a number of controls for the translocation measurements, particularly to support the idea that the fluorescence rise represents ATP-coupled translocation to the 5′-end. In the absence of ATP (or with the nonhydrolyzable analogue AMPPNP instead of ATP), no fluorescence change is observed in the time scale of the translocation if the PcrA·

DNA complex is preformed. If the complex is not preformed, the fluorescence change on binding is observed, followed by a small decrease in fluorescence which we suggest is due to rearrangement of the "random" distribution of PcrA away from the ends. A control was also done with 2AP near the 3′-end of an oligonucleotide which otherwise has all T bases. Using the normal method of oligonucleotide synthesis bound to a resin, 2AP can be incorporated at position 2 but not position 1 of the oligonucleotide. This oligonucleotide only has a very small fluorescence change, which is much more rapid than the time scale of translocation as measured by P_i release (*34*). Finally, this figure shows that the observed fluorescence changes are due to the 2AP, as a measurement in which the 2AP oligonucleotide is replaced with a polythymidylate has much lower fluorescence and there is no fluorescence change.

DISCUSSION

Short oligonucleotides containing single 2AP bases at the 5′-end show fluorescence intensity increases on binding to PcrA. There are then larger increases during the time that the protein undergoes ATP-dependent translocation. Presumably, this signal relates to an enhancement of fluorescence emission when 2AP moves to within the ssDNA binding site of PcrA, and we discuss below how this provides evidence for unidirectional translocation to the 5′-end. The binding site of PcrA consists of several pockets for DNA bases, with aromatic amino acids interacting with the occluded bases (*6*). Translocation data using oligonucleotides containing 2AP in the middle suggest that the fluorescence level may vary depending on which pocket contains the 2AP (M. S. Dillingham, D. B. Wigley, and M. R. Webb, unpublished data). In work presented here, only 5′-2AP DNA is used.

The fluorescence change on DNA binding in the absence of ATP decreases as the oligonucleotide length increases: oligonucleotides of greater than ~30 bases in length produce very little fluorescence increase on binding (Figure 2). Since the measurements are performed under conditions of excess DNA relative to PcrA, this observation is consistent with approximately random binding of the PcrA molecule along the length of the DNA. Other data described above suggest that there may be minor deviations from random binding with complexes at DNA ends somewhat less favored thermodynamically. This results in a slight redistribution away from the ends after initial binding. As suggested with the P_i measurements (*10*), there are between two and four less binding sites than the number of bases.

DNA translocation was investigated using oligonucleotides of various lengths with the 2AP at the 5′-end. These experiments were based on the idea suggested by previous work (*10*) that if ATP-dependent translocation is unidirectional to the 5′-end and dissociation is slow, PcrA molecules will accumulate near this 2AP sensor base in the steady state. Measurements were conducted in which the PcrA was initially free in solution and in which the PcrA·DNA complex was preformed. In all cases, introduction of ATP resulted in fluorescence increasing approximately linearly with time to a maximum and then reducing exponentially as steady state was achieved (Figure 5). As the oligonucleotide length increased, the rate of fluorescence change decreased with a concomitant increase in the time taken to reach maximum fluorescence. Moreover, addition of a DNA chase to sequester PcrA as it dissociates from the 2AP oligonucleotide had very little effect on this early phase of the trace (Figure 4). These observations are consistent with the proposal that this phase represents ATP-dependent DNA translocation and lead to several important conclusions regarding PcrA translocation.

(1) The Translocation Signal Is Consistent with Random Binding. The linear fluorescence increase provides further evidence that PcrA is initially bound at random positions along the oligonucleotides. Because different PcrA molecules start from all positions along DNA, some molecules arrive at the 5′-end soon after translocation is initiated with ATP. Thereafter, they continue to arrive at the same rate until the last molecules (i.e., those which started at the 3′-end and have travelled furthest) have reached the 5′-end. In contrast, if the PcrA molecules were to start in a synchronized manner at the 3′-end of DNA, then the trace would be expected to start with a lag dependent on DNA length. This would be followed by an exponential increase in fluorescence as the molecules reached the 5′-end.

(2) The Fluorescence Signal Is Related to Translocation Speed. The time taken to reach maximum intensity provides a crude estimate of translocation speed. The relationship between time to peak fluorescence and oligonucleotide length is linear with a gradient of 80 bases per second (Figure 6). The kinetics of the fluorescence increase does not in itself provide information on the step size of the helicase; that information was derived from P_i release measurements (*10*).

When the preformed complex was used, the linear fit in Figure 6 intercepts the length axis at ~4. This is equivalent to the length of oligonucleotide for which all the PcrA is bound at the 5′-end at zero time, i.e., when there is only one binding site. This takes into account that there are less available binding sites than the total number of bases and is similar to results from the P_i measurement (*10*) and 2AP oligonucleotide binding (Figure 2). However, using the intercept at zero time does not take into account the fact that, for a short oligonucleotide with a single binding site, there might still be a fluorescence rise after mixing with ATP, concomitant with the proposed conformation change. This is unlikely to be a large factor and is ignored in this analysis.

(3) Translocation Is Unidirectional toward the 5′-End. The linear relationship between oligonucleotide length and the time taken to reach maximum fluorescence (Figure 6) implies that translocation is unidirectional rather than occurring by a random walk. If the latter were true, then the time taken to reach the 5′-terminus would be related to the square of the average distance travelled (*35*). The fit of data in Figure 6 to this model is clearly poor. The data also indicate that the direction of the translocation is 3′ to 5′ since the PcrA molecules must accumulate at or near the 2AP to produce the observed fluorescence increase. When the 2AP was one base from the 3′-end of a 30mer, no ATP-dependent fluorescence changes were observed that lasted over the time scale of the translocation (Figure 7). A 3′−5′ directionality is also consistent with that observed in PcrA helicase assays (*9*).

(4) Translocation Is Processive. The data from binding plus translocation at different oligonucleotide lengths (Figure 5b) show that the final fluorescence intensity is largely unaffected by length. This suggests that most of the PcrA

reaches the 5′-end of DNA for all the lengths studied, i.e., that PcrA is processive on single-stranded DNA. This in turn is consistent with our previous suggestion that PcrA accumulates at the 5′-end of ssDNA. The small difference between maximum fluorescence intensity caused by the chase DNA in Figure 4 may be due to a small amount of protein dissociating during translocation. However, some difference is expected anyway because any protein "waiting" at the 5′-end will dissociate at ~1 s^{-1}. In contrast, during DNA unwinding (i.e., when PcrA has to translocate along ssDNA and invade duplex DNA) processivity is low for PcrA alone (*8*).

(5) PcrA Remains Bound at the 5′-End. After the translocation phase, the fluorescence decreases exponentially to a constant level maintained in the steady state. As described in the Results, the apparent differences in steady-state fluorescence in Figure 5a are due to the way the data are plotted. The fact that this fluorescence is independent of length is consistent with the PcrA largely remaining bound at the 5′-end and dissociating only slowly. The steady-state ATPase rate is also independent of length (*10*), consistent with this idea. There are multiple processes occurring at the 5′-end during this approach to steady state.

Two processes are uncovered by comparing the traces of a translocation measurement with one in the presence of a large excess of chase, unlabeled DNA. In the latter case, PcrA that dissociates from 2AP DNA binds to unlabeled DNA. These measurements show that dissociation occurs at ~1 s^{-1}. However, there is also a process causing a fluorescence decrease at ~2 s^{-1}. Both of these rates are largely independent of DNA length.

On the basis of P_i release measurements (*10*), it was proposed that the dissociation is slow: the modeling gave 0.6 s^{-1}, similar to that measured here. It was also proposed that there is continuing hydrolysis of ATP (at 5.5 s^{-1}) while PcrA remains bound at the 5′-end without translocation. This slow hydrolysis explains the fact that steady-state hydrolysis is independent of DNA length. The process giving rise to the fluorescence change at 2 s^{-1} is too slow to accompany the multiple ATP hydrolysis at 5.5 s^{-1}.

Kinetic Mechanism. We can now add rate constants to the qualitative mechanism described above and illustrated by the cartoon in Figure 8. In some cases particular rate constants vary slightly with length of oligonucleotide (e.g., dissociation). In the first instance we shall ignore these differences but consider such limitations of the modeling later in the discussion.

The kinetics of binding (Figure 1) suggest that there are two steps in this process (steps 1 and 2 in Figure 8), as in eq 1. The maximum rate of 35 s^{-1} of the hyperbola in Figure 1b corresponds to $k_{+2} + k_{-2}$. A value for k_{-2} of 1.3 s^{-1} comes from measurement of the dissociation kinetics in the absence of ATP (Figure 3), so that k_{+2} is 34 s^{-1}. This enables an overall K_d to be calculated for the PcrA·DNA complex, as it is $1/K_1K_2$. This has the value of 73 nM, consistent with the tight binding suggested by steady-state assays (*32*, *36*). We will assume that these values are largely unaffected by the presence of nucleotide, although this is not yet known. Data from Figure 7 suggest that binding has a similar rate with ATP, ADP, or no nucleotide, although the fluorescence changes vary. Binding is assumed to be random along the length of DNA, with the number of sites available being

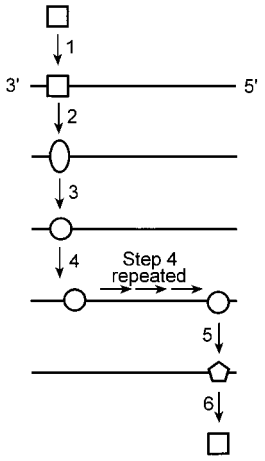

FIGURE 8: Cartoon showing the proposed mechanism of the translocation cycle by PcrA helicase along ssDNA. The line represents ssDNA, and the different shapes represent different conformation states of PcrA and/or PcrA·DNA complexes. Steps 1 and 2 represent the two-step binding as in eq 1. This is followed by an ATP-induced change in conformation (step 3). Translocation then occurs with single base steps (step 4), each requiring one molecule of ATP hydrolyzed. Finally, dissociation occurs in two slow steps. First there is a conformation change (step 5) required to explain the relaxation of the fluorescence traces and then dissociation itself (step 6). The steps are described in detail in the text.

DNA base length minus three. The former is likely to be a simplification as previously mentioned.

In the mechanism of Figure 8, step 3 is a nucleotide-induced conformation change invoked to explain the P_i release data (*10*). It is apparent from the simulations (below) that such a step is also required to obtain optimal fit of the fluorescence data. There is then single base step translocation (step 4) that is repeated until the PcrA reaches the 5′-end: each step involves the hydrolysis of one ATP molecule (*10*). A further conformation change (step 5) occurs corresponding to the exponential decrease in fluorescence during the translocation measurements. Finally, there is slow dissociation (step 6), and the cycle restarts.

Estimates for most of these rate constants come from this work and P_i measurements (*10*), and these were used as a basis for the simulations. However, these individual measurements do not on the whole address the size of specific fluorescence changes during each step, nor do they address how the fluorescence changes as the 2AP moves between base binding pockets i.e., the changes as PcrA translocates along the final few bases at the 5′-end of the DNA.

The simplest assumption would be that only the complex with PcrA bound at the extreme 5′-position has an enhanced fluorescence. However, this could not produce reasonable simulations for two reasons. First, the maximum fluorescence consistently precedes the change from fast to slow phases of P_i release by a small amount of time. Simulations with this assumption have the maximum fluorescence that coincides with the change in P_i release rate. Second, the fluorescence increases during translocation as a function of length were not modeled well. For example, 20_{2AP} binds to PcrA with ~10% fluorescence enhancement (Figure 2). During the translocation phase in Figure 4a it shows a further ~7% fluorescence enhancement. With the simple assumption above and with random binding, the preformed complex at zero time would have ~6% of the fluorescence enhancement

expected if all the PcrA was bound at the 5′-end instead. As the maximum fluorescence in Figure 4 represents the situation when most PcrA is bound at the 5′-end, the model would predict a much larger increase than 7%.

This sort of consideration led to the assignment of a fluorescence contribution from the final three binding sites at the 5′-end. These positions close to the 5′-end are designated, for example, as "5′−2", which refers to PcrA bound two sites in from the final 5′ binding site. The following weightings of the fluorescence intensities, relative to uncomplexed DNA, provide a reasonable fit to data (Figures 4 and 5). No bound adenine nucleotide: PcrA·20_{2AP} (5′−2), 2; PcrA·20_{2AP} (5′−1), 2. With bound adenine nucleotide: PcrA·20_{2AP} (5′−2), 4; PcrA·20_{2AP} (5′−1), 4; PcrA·20_{2AP} (5′), 2. The intermediate formed during step 5 has a relative intensity of 0.2. Because the 5′−2 and 5′−1 sites are only transiently occupied with rapid entry and exit, the fluorescence traces overall are not very sensitive to the individual fluorescence intensities at these positions, only to the sum. This is particularly so for longer oligonucleotides.

Rate constants used in the simulation were k_{+1} 6×10^7 M^{-1} s^{-1}, k_{+2} 34 s^{-1}, k_{+3} 10 s^{-1}, k_{+4} 80 s^{-1}, k_{+5} 2 s^{-1}, and k_{+6} 0.7 s^{-1}. It was assumed that the PcrA could not dissociate from any position on the DNA except from the 5′-end, but in practice that had little effect on the simulations for the lengths shown. Similarly, the value of k_{+1} had little effect. For P_i release simulations, the rate constant for ATP hydrolysis at the 5′-end (not shown in Figure 7) was 5.5 s^{-1}, but this rate constant does not affect the simulations of 2AP fluorescence. The calculated rise from fluorescence for 20_{2AP} at zero time to the maximum value was adjusted to that observed experimentally, and all other simulated curves were adjusted by this same factor to give those in Figures 4 and 5. These simulations reproduce the main features of the experimental traces for the time courses of translocation not only for the 2AP fluorescence but also for the P_i released (*10*) (simulations not shown).

As mentioned above, the set of rate constants used in the simulations were optimized for the 2AP DNA translocation from rate constants for other measurements (binding, release, and P_i). The aim was to get a set of rate constants reasonably consistent with all the types of measurement. One limitation of this approach is that the binding kinetics were measured in the absence of nucleotide, and it is assumed that similar rate constants apply if ATP is present. Thus the modeling has k_{+2} as 34 s^{-1}, the same as that measured experimentally here. Step 1 is given a value of 6×10^7 M^{-1} s^{-1}, although the shape of the simulated curves is not highly dependent on this value. Only a value of K_1 comes from the binding kinetic measurements. In the previous simulations of P_i release (*10*), a somewhat slower rate of translocation was used (50 s^{-1} as compared with 80 s^{-1} here), together with a faster conformation change for step 3 (20 s^{-1}, with 10 s^{-1} here). These changes of rate constant in opposite directions produce small changes in the shape of the fast-phase curves but, overall, compensate for each other, so that the "new" set of rate constants still give reasonable fits to the P_i traces. The simulations suggest that k_{+6} is 0.7 s^{-1}, whereas direct dissociation measurements in the absence of nucleotide give 1.3 s^{-1}.

Limitations of the Kinetic Model. This mechanism gives simulations that reproduce the main features of P_i release (*10*) and the fluorescence changes of 2-aminopurine at the 5′-end of a single strand of DNA during translocation of PcrA. Following random binding and conformational changes, PcrA translocates toward the 5′-end of ssDNA, where it accumulates due to slow dissociation from the terminus (Figure 7). For the P_i release data, the kinetic model provides a good fit to the data, even with the slightly modified numbers presented in this report. The situation is somewhat more complex with the 2AP fluorescence data. The model broadly fits the fluorescence data but is defective in several areas. In general terms, this probably relates to the fact that the 2AP probe is sensitive to various fine effects during translocation which are not described by our simple model. For instance, the shape of the rise in fluorescence during translocation is not predicted well by our model (Figure 5a,c). This is most likely due to the fact that the initial binding event is not completely random but rather that different sites along the oligonucleotides display slightly different affinities for the PcrA molecule. Thus the distribution may differ depending on whether the protein−DNA complex is preformed. If preformed, there may be time for equilibration before ATP addition. If not preformed, the distribution will be largely determined by the kinetics at different binding sites.

The relative increase in fluorescence amplitude observed for different oligonucleotide lengths varies somewhat from that predicted by the model, especially for the 50_{2AP} oligonucleotide. Concentrations for oligonucleotides were calculated by spectrophotometry using theoretical extinction coefficients. In practice, the absolute fluorescence of the different oligonucleotides was similar, but not equal, for equal concentrations of the 2AP base. Therefore, differences in absolute fluorescence may arise as a result of inherent differences in the fluorescent properties of 2AP in oligonucleotides of different lengths or through inaccuracies in concentration determination. However, the time of maximum fluorescence and, consequently, the estimation of translocation speed (Figure 6) are independent of such considerations.

These simulations assume that all rate constants are independent of length. In practice, some rate constants do vary for short oligonucleotides. It has been shown that K_m values for DNA are higher for short (>10) oligonucleotides when measuring the pre-steady-state P_i release (*10*). Here it is shown that the dissociation rate constant is higher by a factor of 2 for the 10mer than longer oligonucleotides, at least from the 5′-end. It is apparent that the 10mer also differs slightly in the position of the transient fluorescence maximum during translocation. This maximum is earlier than the simulation predicts and is very sharp. This is possibly due to alterations in other rate constants due to its short length or end effects becoming significant.

Wider Implications. As a member of helicase superfamily I, PcrA is representative of a large subset of the DNA-based motor proteins. By incorporating 2AP at the 5′-end of standard oligonucleotides of various lengths, we have been able to study the kinetics of ssDNA translocation. Modeling of these kinetic data was achieved with minor quantitative refinements to our existing DNA translocation model based on a study of P_i release from PcrA·DNA complexes (*10*). The fact that both sets of data are resolved by this model provides further confidence in a unidirectional tracking (or inchworm) mechanism for ssDNA translocation by super-

family I DNA helicases. However, it has been proposed that *E. coli* Rep helicase, which is also a member of superfamily I, translocates by DNA looping interactions (*22*, *37*). This forms the basis for an alternative general model for helicase activity termed the "active rolling model" (*2*). Moreover, although helicases of other families may translocate by tracking unidirectionally (*38*, *39*), they do not necessarily employ the base-to-base structural mechanism suggested for PcrA helicase.

Of the DNA translocases whose speed has been examined in detail, PcrA is a somewhat slow and nonprocessive member. The type I restriction enzyme EcoR124I travels at around 400 base pairs per second, covering distances of thousands of base pairs before it dissociates (*15*). Likewise, a molecule of RecBCD is capable of unwinding about 30000 base pairs of DNA at a rate of 1000 base pairs per second (*40*). Since the sequence of RecB, the helicase subunit of RecBCD, is similar to PcrA, it will be intriguing to see how this basic structure has been modified for increased speed and processivity.

Progression of our understanding of helicase activities will require the development of assays that allow the study of the dynamics and forces associated with the protein motion on DNA. This study has extended our understanding of the mechanism of ssDNA translocation in superfamily I DNA helicases. Importantly, the direct nature of the 2-aminopurine assay will open new avenues for the study of PcrA-catalyzed ssDNA translocation. For instance, this assay provides a mechanism for studying the effects of lesions or static blocks on DNA translocation which may be of important physiological significance. It might also allow identification and characterization of mutant proteins with specific defects in DNA translocation, illuminating the mechanism of this molecular motor in structural terms.

ACKNOWLEDGMENT

The authors thank Jennifer Byrne (University of Oxford) and Jackie Hunter (NIMR, London) for technical assistance.

REFERENCES

1. Soultanas, P., and Wigley, D. B. (2000) *Curr. Opin. Struct. Biol. 10*, 124−128.
2. Lohman, T. M., and Bjornson, K. P. (1996) *Annu. Rev. Biochem. 65*, 169−214.
3. Hall, M. C., and Matson, S. W. (1999) *Mol. Microbiol. 34*, 867−877.
4. Gorbalenya, A. E., and Koonin, E. V. (1993) *Curr. Opin. Struct. Biol. 3*, 419−429.
5. McGlynn, P., and Lloyd, R. G. (2000) *Cell 101*, 35−45.
6. Velankar, S. S., Soultanas, P., Dillingham, M. S., Subramanya, H. S., and Wigley, D. B. (1999) *Cell 97*, 75−84.
7. Petit, M. A., Dervyn, E., Rose, M., Entian, K.-D., McGovern, S., Ehrlich, S. D., and Bruand, C. (1999) *Mol. Microbiol. 29*, 261−273.
8. Soultanas, P., Dillingham, M. S., and Wigley, D. B. (1998) *Nucleic Acids Res. 26*, 2374−2379.
9. Bird, L. E., Brannigan, J. A., Subramanya, H. S., and Wigley, D. B. (1998) *Nucleic Acids Res. 26*, 2686−2693.
10. Dillingham, M. S., Wigley, D. B., and Webb, M. R. (2000) *Biochemistry 39*, 205−212.
11. Soultanas, P., Dillingham, M., Wiley, P., Webb, M. R., and Wigley, D. B. (2000) *EMBO J. 19*, 3799−3810.
12. Garcia, L. R., and Molineux, I. J. (1996) *J. Bacteriol. 178*, 6921−6929.
13. Bath, J., Wu, L. J., Errington, J., and Wang, J. C. (2000) *Science 290*, 995−997.
14. Davies, G. P., Kemp, P., Molineux, I. J., and Murray, N. E. (1999) *J. Mol. Biol. 292*, 787−796.
15. Firman, K., and Szczelkun, M. D. (2000) *EMBO J. 19*, 2094−2102.
16. Ellis, D. J., Dryden, D. T. F., Berge, T., Edwardson, J. M., and Henderson, R. M. (1999) *Nat. Struct. Biol. 6*, 15−17.
17. Bianco, P. R., Brewer, L. R., Corzett, M., Balhorn, R., Yeh, Y., Kowalczykowski, S. C., and Baskin, R. J. (2001) *Nature 409*, 374−377.
18. Matson, S. W., and Richardson, C. C. (1983) *J. Biol. Chem. 258*, 14009−14016.
19. Young, M. C., Schultz, D. E., Ring, D., and von Hippel, P. H. (1994) *J. Mol. Biol. 235*, 1447−1458.
20. Brown, W. C., and Romano, L. J. (1989) *J. Biol. Chem. 264*, 6748−6754.
21. Maine, I. P., and Kodadek, T. (1994) *Biochem. Biophys. Res. Commun. 198*, 1070−1077.
22. Amaratunga, M., and Lohman, T. M. (1993) *Biochemistry 32*, 6815−6820.
23. Morris, P. D., and Raney, K. D. (1999) *Biochemistry 38*, 5164−5171.
24. Lee, M. S., and Marians, K. J. (1990) *J. Biol. Chem. 265*, 17078−17083.
25. Sowers, L. C., Fazakerley, G. V., Eritja, R., Kaplan, B. E., and Goodman, M. F. (1986) *Proc. Natl. Acad. Sci. U.S.A. 83*, 5434−5438.
26. Verma, S., and Eckstein, F. (1998) *Annu. Rev. Biochem. 67*, 99−134.
27. Stivers, J. T., Pankiewicz, K. W., and Watanabe, K. A. (1999) *Biochemistry 38*, 952−963.
28. Holz, B., Klimasauskas, S., Serva, S., and Weinhold, E. (1998) *Nucleic Acids Res. 26*, 1076−1083.
29. Allan, B. W., Reich, N. O., and Beechem, J. M. (1999) *Biochemistry 38*, 5308−5314.
30. Furge, L. L., and Guengerich, F. P. (1998) *Biochemistry 37*, 3567−3574.
31. Raney, K. D., Sowers, L. C., Millar, D. P., and Benkovic, S. J. (1994) *Proc. Natl. Acad. Sci. U.S.A. 91*, 6644−6648.
32. Dillingham, M. S., Soultanas, P., and Wigley, D. B. (1999) *Nucleic Acids Res. 27*, 3310−3317.
33. Leatherbarrow, R. J. (1992) *Grafit Version 3.0*, Erithacus Software Ltd., Staines, U.K.
34. Dillingham, M. S., Wigley, D. B., and Webb, M. R. (2001) *Biochemistry* (submitted for publicaton).
35. Grimmett, G. R., and Stirzaker, D. R. (1992) in *Probability and Random Processes*, 2nd ed., pp 73−74, Oxford University Press, Oxford.
36. Soultanas, P., Dillingham, M. S., Velankar, S. S., and Wigley, D. B. (1999) *J. Mol. Biol. 290*, 137−148.
37. Wong, I., and Lohman, T. M. (1996) *Proc. Natl. Acad. Sci. U.S.A. 93*, 10051−10056.
38. Kim, J. L., Morgenstern, K. A., Griffith, J. P., Dwyer, M. D., Thompson, J. A., Murcko, M. A., Lin, C., and Caron, P. R. (1998) *Structure 6*, 89−100.
39. Singleton, M. R., Sawaya, M. R., Ellenberger, T., and Wigley, D. B. (2000) *Cell 101*, 589−600.
40. Arnold, D. A., and Kowalczykowski, S. C. (1999) *Encyclopedia of Life Sciences*, Macmillan Reference Limited, London.

BI011137K